



Spray pyrolysis growth of highly c-Axis oriented Al-doped ZnO thin films for transparent conducting applications

Hanane Chenague ^a, Samir Hamrit ^{a,*}, Abdelhafid Mahroug ^a, Youssef Larbah ^b

^a Laboratory of Materials Physics and Its Applications, Mohamed Boudiaf University of M'sila 28000, Algeria

^b Nuclear Research Center of Algiers (CRNA), 02, Boulevard Frantz Fanon, B.P. 399, Algiers 16000, Algeria

ARTICLE INFO

Keywords:
AZO thin films
Thickness
Spray pyrolysis
RBS, TCOs

ABSTRACT

In this work, a series of 2 at.% Al-doped ZnO (AZO) thin films with thicknesses ranging from 288 to 1040 nm were deposited on glass substrates at 475 °C using spray pyrolysis. X-ray diffraction (XRD) confirmed a highly crystalline wurtzite structure with strong preferential growth along the (002) plane and improved crystallinity with increasing thickness. Rutherford backscattering spectrometry (RBS) verified the targeted Al doping and film thicknesses. Optical measurements showed high transparency, with 80 % transmittance for film-on-substrate samples, corresponding to >90 % intrinsic transmittance of the films alone. Electrical measurements revealed a strong thickness dependence of sheet resistance, decreasing from ~207 Ω/□ for 288 nm films to ~148 Ω/□ for 1040 nm films. These results demonstrate that spray pyrolysis can produce high-quality AZO films with excellent structural, optical, and electrical properties, confirming their strong potential as low-cost transparent conducting oxides (TCOs) for optoelectronic devices.

1. Introduction

Transparent conducting oxides (TCOs) are indispensable in modern optoelectronic devices, including solar cells, flat-panel displays, and touch screens, due to their unique combination of high optical transparency and electrical conductivity [1–3]. Indium tin oxide (ITO) has traditionally dominated this field; however, the escalating cost and limited availability of indium have intensified the search for alternative materials [1]. Zinc oxide (ZnO), with its wide band gap (~3.3 eV), high excitonic binding energy, natural abundance, and environmental benignity, has emerged as a promising candidate [4]. Nevertheless, the intrinsic electrical conductivity of ZnO is insufficient for many applications, necessitating extrinsic doping. Incorporation of group-III elements, particularly aluminum, significantly enhances the carrier concentration, making aluminum-doped ZnO (AZO) a compelling, low-cost TCO alternative [5,6].

AZO thin films can be fabricated by various techniques, such as sputtering, pulsed laser deposition, atomic layer deposition, and spray pyrolysis, each offering distinct advantages in terms of scalability, cost, and film quality [6–9]. While vacuum-based methods like sputtering and pulsed laser deposition yield high-quality films, they require complex and expensive equipment. In contrast, spray pyrolysis is a simple,

scalable, and cost-effective technique suitable for large-area coatings, making it attractive for industrial applications [10].

In this study, we report the synthesis of 2 at.% Al-doped ZnO thin films on glass substrates at 475 °C by spray pyrolysis. The structural, optical, and compositional properties of the films were systematically investigated using X-ray diffraction (XRD), Rutherford backscattering spectrometry (RBS), ultraviolet-visible spectroscopy (UV-Vis) spectroscopy, and photoluminescence (PL). The resulting AZO films exhibited strong c-axis orientation, nanoscale crystallinity, and high optical transparency, underscoring their potential as transparent electrodes for next-generation optoelectronic devices.

2. Experimental details

2.1. Precursor solution preparation and deposition

A 0.1 M precursor solution for 2 at.% Al-doped ZnO (AZO) was prepared by dissolving zinc acetate dihydrate in propanol under stirring for 20 min, followed by the addition of aluminum nitrate nonahydrate to achieve an Al/Zn ratio of 2 %. Ethanolamine was added dropwise as a stabilizing agent to ensure homogeneity. The clear sol was used for spray pyrolysis deposition on glass substrates at 475 °C using a Holmarc HO-

* Corresponding author.

E-mail address: samir.hamrit@univ-msila.dz (S. Hamrit).

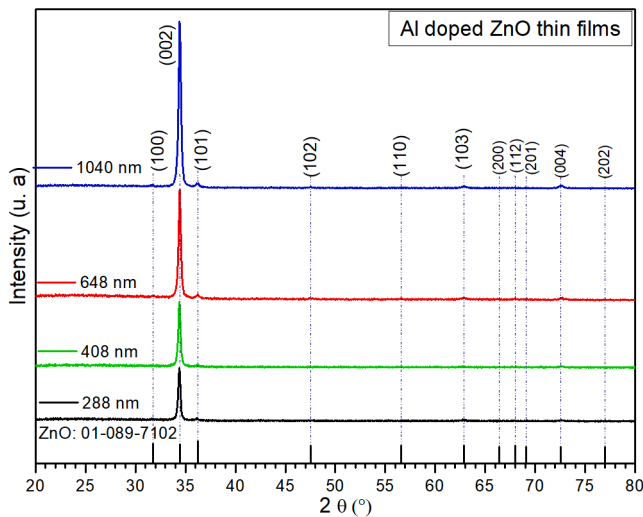


Fig. 1. X-ray diffraction patterns of 2 at.% Al-doped ZnO thin films with different thicknesses deposited by spray pyrolysis, showing highly c-axis oriented growth along the (002) plane.

TH-04 system. Deposition parameters were controlled by an integrated program, maintaining a nozzle-substrate distance of 12 cm, carrier gas pressure of 30 psi, and solution flow rate of 2 ml/min. Film thickness was adjusted by deposition time and confirmed by RBS and optical analysis.

2.2. Thin film characterization

The crystal structure was characterized by X-ray diffraction using an X'Pert PRO PANalytical diffractometer ($\text{Cu K}\alpha$, $\lambda = 1.5418 \text{ \AA}$, 40 kV, 30 mA, 0-2θ mode). Optical transmittance (200–800 nm) was measured using a Shimadzu UV-2401 PC spectrophotometer. Photoluminescence (PL) spectra were acquired at room temperature with a Perkin-Elmer LS-50B luminescence spectrometer using a 325 nm Xenon lamp excitation source. The sheet resistance of the thin films was measured at room temperature using a standard four-point probe system. The elemental composition and film thickness were accurately determined by Rutherford backscattering spectrometry (RBS) using a 2.0 MeV He^+ ion beam.

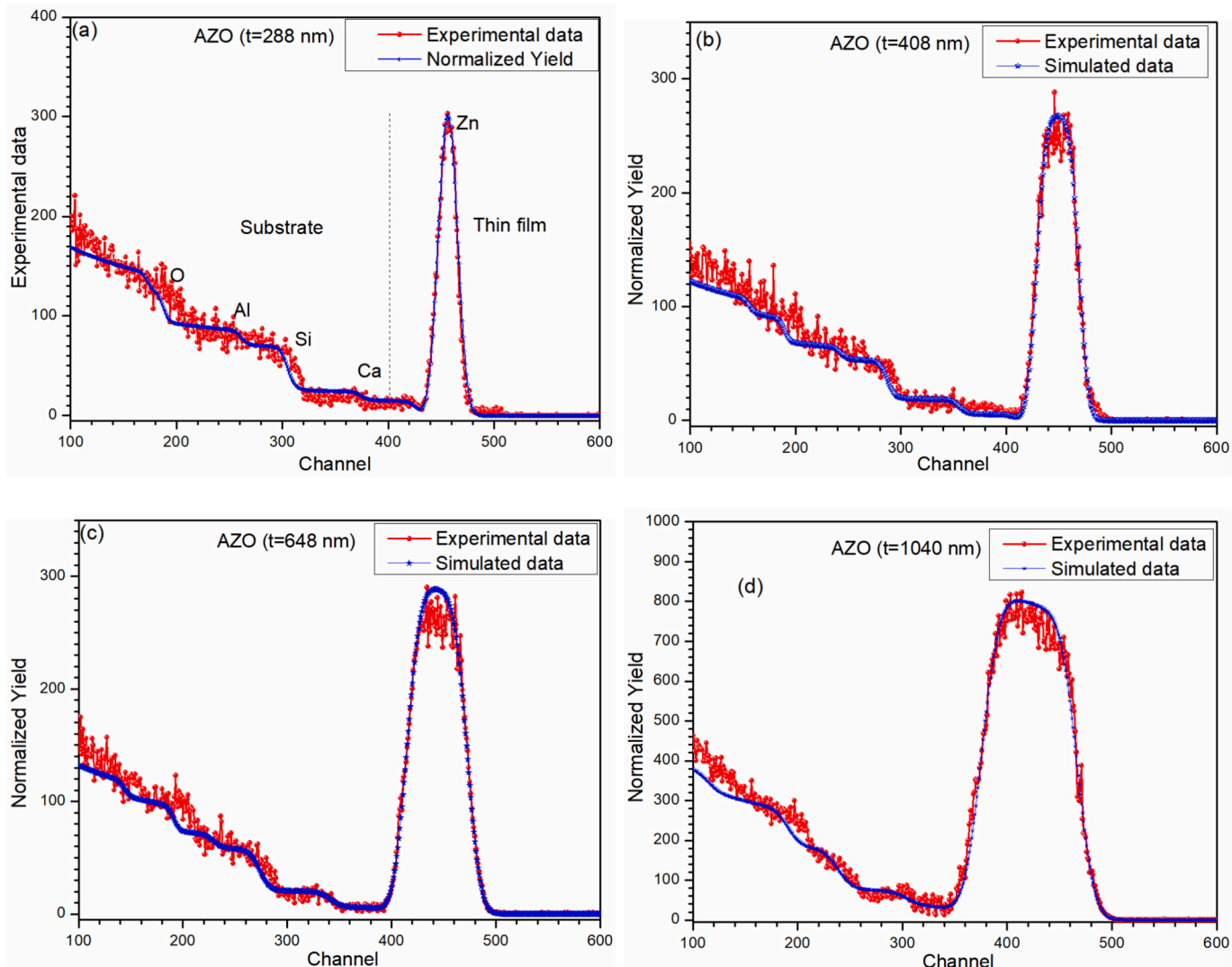


Fig. 2. Rutherford backscattering spectra of AZO thin films with different thicknesses, confirming the intended 2 at.% Al doping and accurate thickness determination.

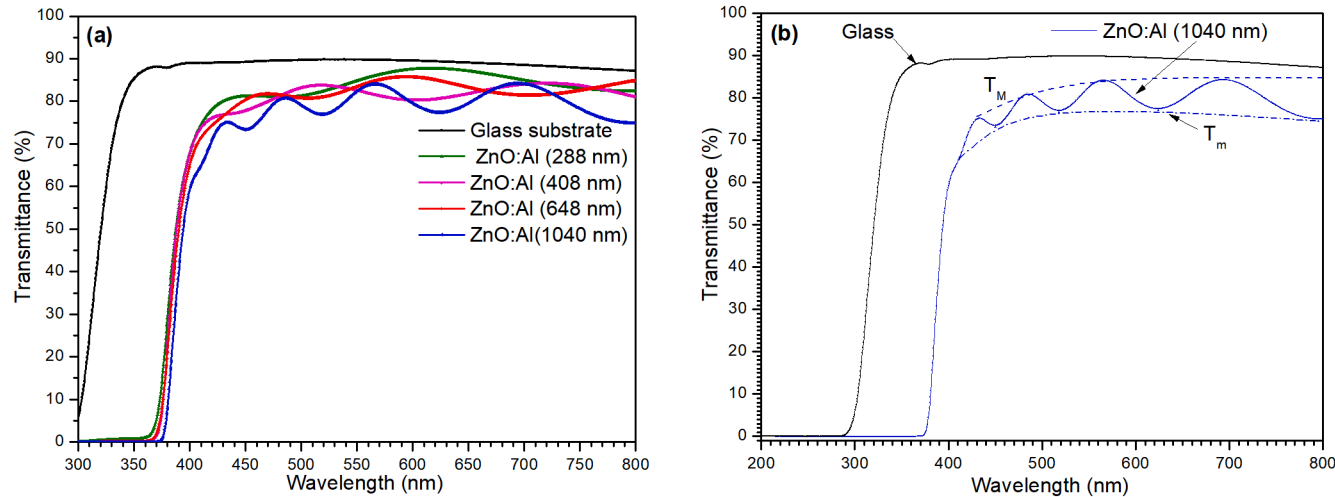


Fig. 3. (a) Optical transmittance spectra of AZO thin films with varying thicknesses. (b) Spectrum of the thicker film showing clear interference fringes.

3. Results and discussion

3.1. X-ray diffraction analysis

Fig. 1 presents the X-ray diffraction (XRD) patterns of 2 % Al-doped ZnO (AZO) thin films deposited with varying thicknesses. All patterns are indexed to the hexagonal wurtzite structure of ZnO (JCPDS card no. 01-089-7102), confirming the successful formation of the desired crystal phase. The most prominent feature is the intense and sharp diffraction peak observed at approximately $2\theta = 34.4^\circ$, which corresponds to the (002) plane. The overwhelming dominance of this peak indicates a strong preferential growth orientation, with the c-axis of the crystals aligned perpendicular to the substrate surface.

Notably, the degree of preferential c-axis orientation observed in our films is exceptionally high. The XRD pattern, characterized by a dominant (002) peak with extremely suppressed non-(00l) reflections, is of a quality that is typically associated with sophisticated vacuum-based deposition techniques such as sputtering and pulsed laser deposition (PLD) [11,12]. The texture coefficient (TC), calculated off-line using reference intensities from JCPDS 01-089-7102, yielded TC (002) ≈ 2.783 (288 nm), 2.838 (408 nm), 2.822 (648 nm), and 2.903 (1040 nm), confirming strong c-axis orientation. Achieving such texture and crystallinity through spray pyrolysis-a cost-effective, and scalable chemical method is rare and underscores the efficiency of our optimized deposition parameters. This orientation arises from surface-energy minimization during growth, favoring the thermodynamically stable (002) basal plane [13].

Fig. 2(a-d) shows the Rutherford Backscattering Spectrometry (RBS) spectra of 2 at.% Al-doped ZnO thin films on glass with thicknesses of 288, 408, 648, and 1040 nm. Each spectrum exhibits distinct Zn and Al surface signals, a broad O region, and substrate peaks from Si, Na, and Ca in the glass. Simulated profiles based on a single-layer AZO model fit the data well, confirming uniform Al distribution and near-stoichiometric Zn:O composition. The RBS-derived thicknesses increase systematically with deposition time (288–1040 nm), matching optical results. The consistent fits without interfacial diffusion or compositional gradients demonstrate the excellent uniformity and controlled growth of the spray-pyrolyzed AZO films. Furthermore, the single-layer simulation confirms that the uniform Al concentration is maintained throughout the entire film depth, with no evidence of segregation or depth-dependent variation in composition.

3.2. Electrical properties

The electrical properties of the AZO thin films were evaluated using a

standard four-point probe method at room temperature. The measured sheet resistance values for the films with thicknesses of 288, 408, 648, and 1040 nm were approximately 207, 185, 162, and $148 \Omega/\square$, respectively. The results clearly show that the sheet resistance decreases with increasing film thickness, which can be attributed to improved crystallinity and grain connectivity, leading to enhanced carrier transport and reduced grain boundary scattering in thicker films.

3.3. Optical properties

Fig. 3(a) presents the optical transmittance spectra of the bare glass substrate and the 2 at.% Al-doped ZnO (AZO) thin film deposited on glass. The bare glass exhibits a smooth transmittance of approximately 85–90 % throughout the visible region. After deposition, the AZO-coated substrate retains high transparency, with an average transmittance of around 80 %. Considering the optical contribution of the glass substrate, the intrinsic transmittance of the AZO film itself exceeds 90 %, confirming its excellent optical quality. The periodic interference fringes observed in the AZO/glass spectrum indicate uniform film thickness and smooth surface morphology. These results further support the potential of the spray-pyrolyzed AZO films as promising candidates for transparent electrode applications.

Fig. 3(b) shows the optical transmittance spectrum of the thicker 2 at.% Al-doped ZnO film on glass. The periodic interference fringes in the visible region arise from multiple reflections in the uniform, transparent AZO layer and were analyzed by the Swanepoel method [14]. The refractive index (n) in the transparent region (λ (wavelength) > 500 nm) was obtained from:

$$n = \left[N + (N^2 - n_s^2)^{1/2} \right]^{1/2}$$

With

$$N = 2n_s \frac{T_M - T_m}{T_M T_m} + \frac{n_s^2 + 1}{2}$$

and $n_s \approx 1.5$ for glass.

For each pair of adjacent maxima (or minima) at wavelengths λ_1 and λ_2 , the film thickness d was obtained from

$$d = \frac{\lambda_1 \lambda_2}{2(\lambda_1 n_2 - \lambda_2 n_1)}$$

where n_1 and n_2 are the refractive indices calculated at λ_1 and λ_2 , respectively.

The average optical thickness (~ 1040 nm) agrees closely with the

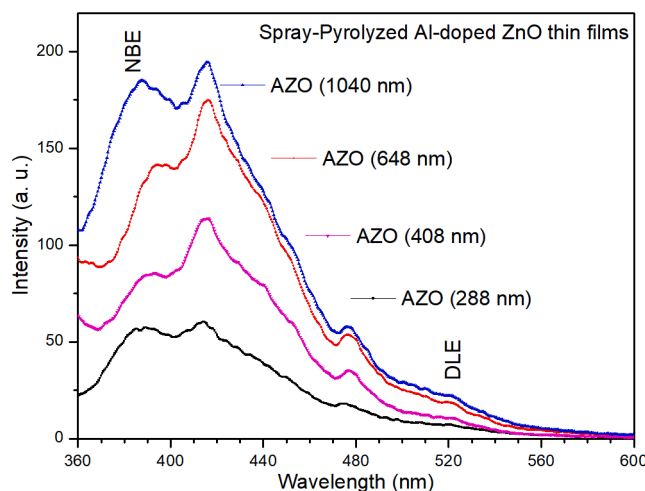


Fig. 4. Room-temperature photoluminescence spectra of AZO thin films of different thicknesses under 325 nm excitation, showing dominant near-band-edge emission and suppressed deep-level emission.

RBS result, confirming the uniformity and high optical quality of the spray-pyrolyzed AZO coatings.

Fig. 4 illustrates the room-temperature photoluminescence spectra of AZO thin films deposited with different thicknesses under 325 nm excitation. All films exhibit a strong and sharp near-band-edge (NBE) emission peak in the ultraviolet region (~385 nm), which is attributed to free excitonic recombination in ZnO [15]. The intensity of this peak increases with increasing film thickness, consistent with the XRD results indicating enhanced crystallinity and grain size in thicker films. In contrast, the broad deep-level emission (DLE) band in the visible region, typically associated with oxygen vacancies and zinc interstitials [16], is strongly suppressed in all samples. The high intensity ratio of NBE to DLE emission highlights the excellent optical quality of the spray-pyrolyzed AZO films, consistent with recent studies showing that Al doping enhances NBE emission while suppressing deep-level defects [17]. These results further demonstrate the suitability of the films for optoelectronic and transparent conducting applications.

4. Conclusion

High-quality 2 % Al-doped ZnO thin films with varying thicknesses were successfully deposited on glass substrates via spray pyrolysis at 475 °C. All thin films are highly c-axis oriented with a hexagonal wurtzite structure. The crystallinity and grain size improve significantly with increasing film thickness. RBS confirms the successful incorporation of Al at the intended doping level and provides accurate thickness calibration. The thin films are highly transparent (>80 %) in the visible region. The PL spectra are dominated by a strong near-band-edge emission, confirming excellent optoelectronic quality. The thicker AZO films (1040 nm) prepared in this study, combining high crystallinity, excellent transparency, and good stoichiometric control, demonstrate strong potential for use as efficient transparent electrodes in various optoelectronic applications.

CRediT authorship contribution statement

Hanane Chenague: Writing – original draft, Investigation, Data curation. **Samir Hamrit:** Writing – review & editing, Validation, Supervision, Project administration, Methodology, Investigation, Data curation. **Abdelhafid Mahroug:** Writing – review & editing, Data curation. **Youssef Larbah:** Writing – review & editing, Formal analysis, Data curation.

Declaration of competing interest

The authors declare that they have no known competing financial interests or personal relationships that could have appeared to influence the work reported in this paper.

Acknowledgements

The authors gratefully acknowledge the financial support provided by the Algerian Ministry of Higher Education and Scientific Research (MESRS) through the PRFU project (B00L02UN280120230010).

Data availability

Data will be made available on request.

References

- [1] J. Patel, et al., Nanomaterials 14 (2024) 2013, <https://doi.org/10.3390/nano14242013>.
- [2] A. Crossay, et al., Sol. Energy Mater. Sol. Cells 101 (2012) 283–288, <https://doi.org/10.1016/j.solmat.2012.02.008>.
- [3] W. Cao, et al., J. Photonics Energy 4 (2014) 040990, <https://doi.org/10.1111/j.1.jpe.4.040990>.
- [4] F.T.Z. Toma, et al., Discov. Mater. 5 (2025) 60, <https://doi.org/10.1007/s43939-025-00201-1>.
- [5] Y. Wu, et al., J. Mater. Sci. Mater. Electron. 31 (2020) 17365–17374, <https://doi.org/10.1007/s10854-020-04292-9>.
- [6] O. Alev, et al., Surf Interfaces 52 (2024) 104942, <https://doi.org/10.1016/j.surfin.2024.104942>.
- [7] S. Hamrit, et al., J. Mater. Sci. Mater. Electron. 27 (2016) 1730–1737, <https://doi.org/10.1007/s10854-015-3947-6>.
- [8] G. Kaur, et al., Prog. Nat. Sci. Mater. Int. 25 (2015) 12–21, <https://doi.org/10.1016/j.pnsc.2015.01.012>.
- [9] H. Ftouhi, et al., Eur. Phys. J. Appl. Phys. 87 (2019) 11101, <https://doi.org/10.1051/epjap/2019190111>.
- [10] H.Q.N.M. Al-Arique, et al., Opt. Mater. 150 (2024) 115261, <https://doi.org/10.1016/j.optmat.2024.115261>.
- [11] A. Collado-Hernández, et al., Thin Solid Films 825 (2025) 140753, <https://doi.org/10.1016/j.tsf.2025.140753>.
- [12] R. Thangavel, et al., J. Phys. Chem. Solids 74 (2013) 1533–1537, <https://doi.org/10.1016/j.jpcs.2013.05.020>.
- [13] H.Q.N.M. AL-Arique, et al., Opt. Mater. (Amst). 150 (2024) 115261, <https://doi.org/10.1016/j.optmat.2024.115261>.
- [14] J. Sánchez-González, et al., Appl. Surf. Sci. 252 (2006) 6013–6017, <https://doi.org/10.1016/j.apsusc.2005.11.009>.
- [15] T.M.K. Thandavan, et al., PLoS One 10 (2015) e0121756, <https://doi.org/10.1371/journal.pone.0121756>.
- [16] A. Galdámez-Martínez, et al., Nanomaterials 10 (2020) 857, <https://doi.org/10.3390/nano10050857>.
- [17] Z. Li, et al., Phys. B Condens. Matter 717 (2025) 417788, <https://doi.org/10.1016/j.physb.2025.417788>.